

# Discriminative Region Proposal Adversarial Networks for High-Quality Image-to-Image Translation

Chao Wang Haiyong Zheng Zhibin Yu Ziqiang Zheng Zhaorui Gu Bing Zheng  
Ocean University of China  
Qingdao, China

## Abstract

Image-to-image translation has been made much progress with embracing Generative Adversarial Networks (GANs). However, it's still very challenging for translation tasks that require high-quality, especially at high-resolution and photo-reality. In this paper, we present Discriminative Region Proposal Adversarial Networks (DRPANs) with three components: a generator, a discriminator and a reviser, for high-quality image-to-image translation. To reduce the artifacts and blur problems while translation, based on GAN, we explore a patch discriminator to find and extract the most artificial image patch by sliding the output score map with a window, and map the proposed image patch onto the synthesized fake image as our discriminative region. We then mask the corresponding real image using the discriminative region to obtain a fake-mask real image. For providing constructive revisions to generator, we propose a reviser for GANs to distinguish the real from the fake-mask real for producing realistic details and serve as auxiliaries to generate high-quality translation results. Experiments on a variety of image-to-image translation tasks and datasets validate that our method outperforms state-of-the-art translation methods for producing high-quality translation results in terms of both human perceptual studies and automatic quantitative measures.

## 1. Introduction

Why we take a synthesized image as fake is often because it includes local artifacts. Although it looks like a real sample in the first glance, we can still easily tell the fake from real with gazing for about only 1000ms. Human artists have the ability to draw a real scene from a given structure like buildings and rooms. They can not only get the global structure of scenes, but also have the ability to focus on the details of the objects and how it is associated with surroundings. So can we build an intelligent system for this task?

Many efforts have been made to develop an automatic image-to-image translation system. The straightforward ap-

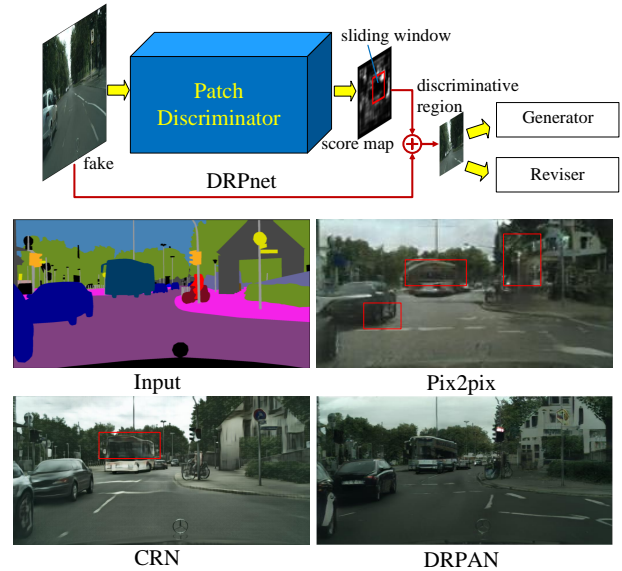


Figure 1: **Top:** Our Discriminative Region Proposal network (DRPnet). **Bottom:** Synthesized samples compared with previous works on Cityscapes validation dataset [6]. The regions within red window show obvious artifacts or deformation. Our method can synthesize images with clear structure and vivid details.

proach is to optimize on pixel-wise space with L1 or L2 loss [9, 23]. However, both of them suffer from blur problem. So considering the blur problem caused by L1/L2 loss, some works have attempted to add adversarial loss which can generate more sharp image in both spatial and spectral dimensions [14]. Except for the GAN loss, some works present perceptual loss as an evaluation, which is often used in neural style translation tasks. It is limited to a pre-training model and the training database. However, using GAN for image translation tasks still encounters with the artifacts and unsmooth color distribution problems, and it is even hard to generate large resolution photo-realistic images because of the high dimension distribution.

Now, it's not a problem of asking can we build an in-

telligent system for image-to-image translation tasks, but a problem of asking how it can perform like a human artist. In this paper, we improve the translation tasks for synthesizing high-quality images via Discriminative Region Proposal Adversarial Network (DRPAN, see Fig. 1 for illustration and example). Our framework is based on patch-wised Discriminative model to predict the discriminative score map by sliding windows to find the most artificial region. Then the proposed discriminative region will be used to mask the corresponding real samples and output as “fake-mask real”. Finally, we propose a reviser to distinguish the real from the fake-mask real for producing realistic details and serve as auxiliaries for generator to synthesize high-quality translation results. Besides, to overcome the high dimension distribution approximation and unstable training problems, we combine our DRPAN with gradient penalty learning. Furthermore, we provide a weighted parameter to balance the contribution of the patch discriminator and our reviser for different levels of translation tasks (see Sec. 4). With this proposed DRPAN, we can synthesize high-quality images with high-resolution and photo-reality but less artifacts.

The main contribution of the study is threefold: first, we design the mechanism to explore GANs for extracting discriminative region; second, we propose the reviser for GANs to produce constructive revisions for generator; third, we build a DRPAN model as a general-purpose solution for high-quality image-to-image translation tasks on different levels.

## 2. Related work

**Feed-forward based approach.** Deep Convolutional Neural Networks (CNNs) have been performed well on many computer vision tasks. For style transform problems [15], many studies are mainly based on VGG-16 network architecture [20] and use perceptual losses for style translation [10]. Network architectures that work well on object recognition tasks have been proved to work well on generative models, for example, some computer vision translation and editing tasks use residual block as a strong feature learning representation architecture [19, 22]. Feed-forward CNNs accompanied with per-pixel loss have been presented for image super-resolution [9, 16, 33, 15], image colorization [8, 42], and semantic segmentation [23, 4, 30]. A recent work for photo realistic image synthesis system, called CRN [5], can synthesize images with high resolution. However, the images synthesized by feed-forward based approach usually become smooth too much rather than realistic, for example not sharp enough in details. Besides, these methods are limited to be used to other image-to-image translation tasks.

**GAN based approach.** GANs [11] introduced an unsupervised method to learn real data distribution. DC-GAN [28] firstly used CNNs to train generative adver-

sarial networks which was hard to be deployed in other tasks before. Then, CNNs were extensively used for designing GAN architectures. Towards stable training of GAN, WGAN [1] replace Jensen-Shannon divergence by Wasserstein distance as the optimization metric, and recently a variety of more stable alternatives have been proposed [27, 18, 12]. Wang and Gupta [37] combined structured GAN and style GAN to learn to generate natural indoor scenes. Reed *et al.* [29] used text as conditional input to synthesize images with semantic variation. Pathak *et al.* [26] proposed context encoders for image inpainting accompanied by adversarial loss. Li *et al.* [21] trained GANs with a combination of reconstruction loss, two adversarial losses and a semantic parsing loss for face completion. Nguyen *et al.* [25] presented Plus and Play Generative Networks for high-resolution and photo-realistic image generation with the resolution of  $227 \times 227$  images. Isola *et al.* explored [14] conditional GANs for a variety of image-to-image translation problems. ID-CGAN [41] combined conditional GANs with perceptual loss for single image de-raining and de-snowing. Considering that the paired images are less and hard to collect, some works gave unpaired or unsupervised translation frameworks as solutions [44, 17, 39]. But it limits to how same of the translation between domain  $A$  and domain  $B$ .

PatchGAN was firstly used in neural style transfer with CNNs based on patch feature inputs [20]. Pix2pix [14] showed that a full ImageGAN does not show quality improvement compared with a low  $70 \times 70$  patch discriminator which has less parameters and needs low computing resource. SimGAN [34] used patch based score map for real image synthesis tasks and mapped a full image to a probability map. Our method explores PatchGAN to a unified discriminative region proposal network model for deciding where and how to synthesize via a reviser. We show that this approach can improve translation results on high-quality, especially at high-resolution and photo-reality.

## 3. Method

Our image-to-image translation model, called Discriminative Region Proposal Adversarial Networks (DRPANs), is composed of three components: a generator, a discriminator, and a reviser. The discriminator explores PatchGAN to construct Discriminative Region Proposal network (DRPnet, see Fig. 1 for reference) to find and extract the discriminative region for producing fake-mask real sample, while the reviser adopts CNN to distinguish the real from the fake-mask real to provide constructive revisions for the generator. The overall network architecture and data flow are illustrated in Fig. 2.

Fig. 3 shows the process of our method to improve the quality of synthesized image. It can be seen that, as our DRPAN continues to train, the discriminative region for fake-

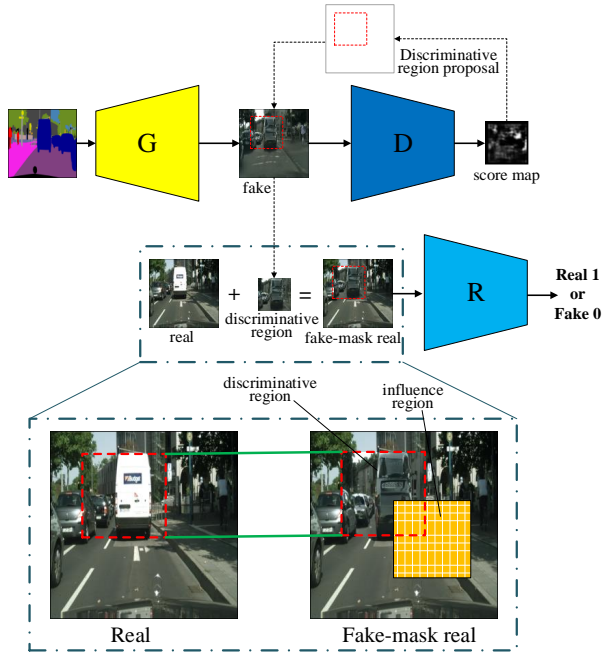


Figure 2: The overall network architecture and data flow of our proposed Discriminative Region Proposal Adversarial Network (DRPAN), which is composed of three components: a generator, a discriminator, and a reviser, and is a unified model for image-to-image translation tasks.

mask real images (top) varies so that the quality of synthesized images (bottom) is improved with brighter score map (right near the first and the last). Besides, although it is hard to distinguish the synthesized sample from the real sample after many epochs, our DRPAN can still revise the generator to optimize the synthesized result in the details for high-quality.

### 3.1. DRPAN

For the primary intuition, we show the output results of score map on different quality levels of images by a pre-trained PatchGAN in Fig. 4. It can be seen that, the score map in the first row is the output of the fake sample in the same row, which has obvious artifacts and shape deformation on some regions, so that the corresponding regions in the score map are almost dark with the lowest score; in contrast, the fake sample in the second row looks better with higher quality than the first one, so the corresponding score map also looks brighter; while, the score map in the third row showing the brightest with the highest score is actually the output of the real sample. From the visualization of score maps, we can calculate to find the darkest region for proposing the discriminative region that indicates the remarkable fake region.

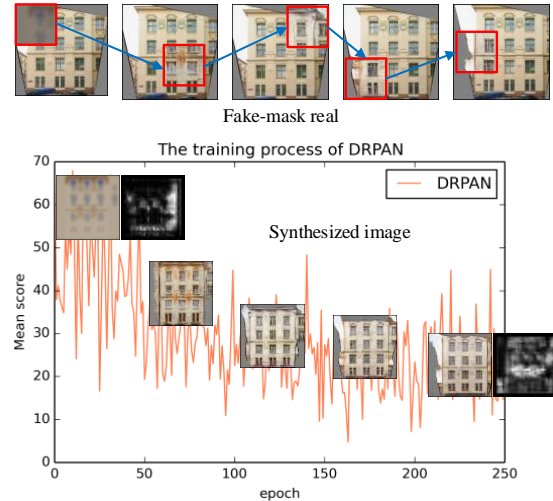


Figure 3: The training process of DRPAN on facades dataset [35]. **Top:** Step by step synthesis on different discriminative regions. **Bottom:** The plotting shows mean value of score map on synthesized samples.

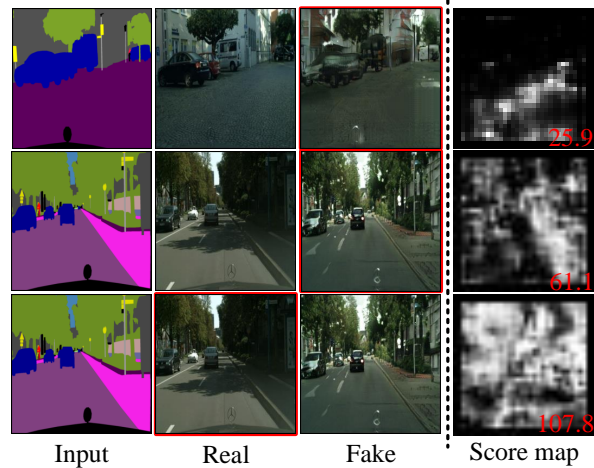


Figure 4: The output results of score map on different quality levels of images by a pre-trained PatchGAN. The last column of score maps are the corresponding output results of the images within red box in the same row. The darkest region on score map indicates the lowest quality on input image, so that PatchGAN can be explored for discriminative region proposal.

Based on the observation shown in Fig. 4, we explore the patch discriminator to DRPnet for producing discriminative region. Given an input image with resolution  $w_i \times w_i$ , and it is processed by the patch discriminator to be a probability score map with size  $w_s \times w_s$ . Suppose we want to obtain the

discriminative region at  $w^* \times w^*$ , the size of sliding window  $w$  for score map can be calculated by

$$w = w^* \times w_s / w_i. \quad (1)$$

Then our DRPnet will find the discriminative square patch on score map with the center coordinates  $(x_c, y_c)$  and length  $w$ , so the scale  $\tau$  between the input image and output score map is

$$\tau = \frac{w_i - w^*}{w_s - w}. \quad (2)$$

The center coordinates  $(x_c^*, y_c^*)$  of discriminative region will be calculated by

$$\begin{cases} x_c^* = \tau \times x_c, \\ y_c^* = \tau \times y_c. \end{cases} \quad (3)$$

Finally, the discriminative region  $d_r$  produced by DRPnet can be expressed as

$$d_r = F_{\text{DRPnet}}(x_c^*, y_c^*, w^*) \quad (4)$$

Instead of only optimizing the independent local regions, we consider the relationship between fake discriminative region and real surrounding influence regions, so that it can connect the fake to the real for providing constructive revisions to generator. For this purpose, we mask the corresponding real sample using the fake discriminative region to make the fake-mask real sample, and then design a reviser using CNN to distinguish the real from the fake-mask real to optimize the generator for synthesizing high-quality images. The reviser we proposed can also be used for other GANs to improve the quality of generated samples.

### 3.2. Objective

For image-to-image translation tasks, we not only want to generate the realistic sample, but also desire diversity with different conditional inputs. The original GAN suffers from the instability and mode collapse problems [1, 2]. So some recent works [1, 27, 12] have improved the training of GAN. To stable training our DRPAN with high-diversity synthesis ability, we modify DRAGAN [18] as the loss of patch discriminator  $D_p$

$$\begin{aligned} \mathcal{L}_D(G, D_p) = & \mathbb{E}_y[\log D_p(x, y)] \\ & + \mathbb{E}_{x,z}[\log(1 - D_p(x, G(x, z)))]. \end{aligned} \quad (5)$$

For reviser  $R$ , to distinguish between the very similar real and fake-mask real  $y_{\text{mask}} = M(G(x, z))$  ( $M(\cdot)$  represents the mask operation), we add a regularization to the loss of reviser as the penalty, which is expressed as

$$\begin{aligned} \mathcal{L}_R(G, R) = & \mathbb{E}_y[\log R(x, y)] + \mathbb{E}_{x,z}[\log(1 - R(x, y_{\text{mask}}))] \\ & + \alpha \mathbb{E}_{x,\delta}[\|\nabla_x R(x + \delta)\| - 1]^2, \end{aligned} \quad (6)$$

where  $\alpha$  is a hyper parameter,  $\delta$  is random noise on  $x$ , and  $\nabla$  indicates the gradient.

Previous studies have found it beneficial to mix the GAN objective with a more traditional loss, such as L2 and L1 distance [14, 34]. Considering that L1 distance encourages less blurring than L2 [14], we provide extra L1 loss for regularization on the whole input image and the local discriminative region to generator, which is defined as

$$\begin{aligned} \mathcal{L}_{L_1}(G) = & \beta \mathbb{E}_{x,y,z}[\|y - G(x, z)\|_1] \\ & + \gamma \mathbb{E}_{d_r,y_r,z}[\|y_r - F_{\text{DRPnet}}(G(x, z))\|_1], \end{aligned} \quad (7)$$

where  $\beta$  and  $\gamma$  are hyper parameters,  $d_r$  is the discriminative region, and  $y_r$  represents the region on the real image corresponding to the discriminative region on the synthesized image. Then the total loss of generator can be expressed as

$$\begin{aligned} \mathcal{L}_G(G, D_p, R) = & -\mathbb{E}_{x,z}[\log(1 - D_p(x, G(x, z)))] \\ & - \mathbb{E}_{x,z}[\log(1 - R(x, y_{\text{mask}}))] + \mathcal{L}_{L_1}(G). \end{aligned} \quad (8)$$

Our proposed model totally contains a generator  $G$ , a patch discriminator  $D_p$  for DRPnet, and a reviser  $R$ .  $G$  will be optimized by  $D_p$ ,  $R$  and  $L_1$ . And our full objective function is

$$L(G, D_p, R) = (1-\lambda)\mathcal{L}_D(G, D_p) + \lambda\mathcal{L}_R(G, R) + \mathcal{L}_{L_1}(G), \quad (9)$$

where  $\lambda$  is a hyper parameter to balance  $\mathcal{L}_D$  and  $\mathcal{L}_R$ .

### 3.3. Network architecture

For our generator, we use architecture based on [19] which has convincing power for single image super-resolution. We adopt convolution and fractionally convolution blocks for down sampling and up sampling respectively, and 9 residual blocks [44] for task learning. And each layer uses batch normalization [13] and ReLU [24] as activation function. For the patch discriminator, we mainly implement with  $70 \times 70$  PatchGAN [20, 14]. The DRPAN reviser is a discriminator modified on DCGAN [28] which has a global view on the whole input. At the end of both patch discriminator and reviser, we adopt Sigmoid as activation function to output probability. We also deploy the model with more residual blocks and discriminative layers for high-quality image-to-image translation tasks.

### 3.4. Training procedure

We learn DRPAN parameters by minimizing the  $\mathcal{L}(G, D_p, R)$ . We employ mini-batch SGD and apply Adam optimizer. To learn the difference between fake-mask real and real, the reviser adds gradient penalty as an alternative regularization scheme, which enforce that reviser parameters are lipschitz in  $x$ . The hyper parameter  $\alpha$  is set to 10 which we found to work robust across a variety of datasets.



We set the number of  $k$  steps to 1 and assign mini-batch size to  $1 \sim 4$  in different tasks. The full adversarial training procedure of our DRPAN is shown in Alg. 1.

---

**Algorithm 1** Adversarial training of DRPAN.

---

**Input:** Input images  $x_i \in \mathcal{X}$ , and paired real images  $y_i \in \mathcal{Y}$   
**Require:** The width of sliding window  $w$ , the parameter  $\lambda$  to balance  $\mathcal{L}_D$  and  $\mathcal{L}_R$ , the proposed region scale  $\tau$ , DRPAN with generator parameters  $\theta$ , patch discriminator parameters  $\omega_D$ , and reviser parameters  $\omega_R$ .

- 1: **while**  $\theta$  has not converged **do**
  - 2:   **for**  $k$  steps **do**
  - 3:     Sample a mini-batch of input images  $x_i$ , and paired images  $y_i$
  - 4:     Update  $\omega_D$  by Adam optimizer on mini-batch with  $\mathcal{L}_D$  in Eqn. 5.
  - 5:     Predict mini-batch of score map by  $D_p$
  - 6:     Propose mini-batch of  $d_r$  by Eqn. 4
  - 7:     Mask real images  $y_i$  by  $M(\cdot)$  to obtain  $y_{\text{mask}}$
  - 8:     Update  $\omega_R$  by Adam optimizer on mini-batch with  $\mathcal{L}_R$  and gradient penalty in Eqn. 6.
  - 9:   **end for**
  - 10:   Update  $\theta$  by taking Adam optimizer on mini-batch in Eqn. 8
  - 11: **end while**
- 

## 4. Experiments

To evaluate the performance of our proposed method on image-to-image translation tasks, we deploy a variety of experiments about different levels of translation tasks to compare our method with state-of-the-arts. And for different tasks, we also use different evaluation metrics including human perceptual studies and automatic quantitative measures.

### 4.1. Evaluation metrics

**Image quality evaluation.** PSNR, SSIM [38] and VIF [32] are some of the most popular evaluation metrics in some low-level computer vision tasks such as deblurring, dehazing and image restoration. So for de-raining and aerial to maps tasks, we adopt PSNR, SSIM, VIF and RECO [3] to qualify the performance of results.

**Image segmentation evaluation metrics.** We use the standard metrics from Cityscapes benchmark [6] to evaluate real to semantic labels task on Cityscapes dataset. The metrics include per-pixel accuracy, per-class accuracy, and Class IOU.

**Amazon Mechanical Turk (AMT).** AMT [14, 44, 39] is adopted in many tasks as a gold metric to evaluate how real the synthesized images, and we use it as evaluation metric for semantic labels to photo and maps to aerial tasks.

**FCN-8s score.** Now, it’s also popular to use automatic quantitative measures such as fully convolutional semantic segmentation networks for quality evaluation of generated images [34, 43]. The intuition is that if the generated images are realistic, classifiers trained on real images will be able to classify the synthesized image correctly as well [14].



Figure 5: Example results of our DRPAN with different sizes of discriminative region compared to ID-CGAN [41] on single image de-raining task.

We use the popular FCN-8s score [23] to evaluate semantic labels to real task on Cityscapes dataset. The FCN-8s model trained on Cityscapes segmentation tasks is taken from [14].

**Inception score.** Inception score is first proposed in [31] and is taken as a diversity evaluation of GAN model. It is also an automatic method to evaluate samples and is well correlated with human evaluation of diversity. So we use inception score as an evaluation metric for abstract to real tasks, which requires diversity evaluation very much.

### 4.2. Low level translation

We first apply our model on two low level translation tasks which are only related to the appearance translation of images, for example, in de-raining task we don’t need change the content and texture of the input sample. So we set  $\lambda = 1$  in Eqn. 9 for image synthesis using only reviser.

**Single image de-raining.** We trained and tested our DRPAN model on single image de-raining task using the procedure as same as [41], and evaluated the results by both qualitative and quantitative metrics. Fig. 5 shows the qualitative results of our DRPAN with different sizes of discriminative region compared to ID-CGAN [41], and our DRPAN outperforms ID-CGAN with not only more effective de-raining but also more vivid color and clear details. Tab. 1 reports the corresponding quantitative results evaluated by PSNR, SSIM, VIF, and RECO metrics, and the best results (in bold font) are achieved all by our DRPAN.

**Bw to color.** We trained our DRPAN model for image colorization task on two datasets: SUN6 [8] and ImageNet [7], and tested on SUN6 dataset with an example shown in Fig. 6. It can be seen that our DRPAN also synthesized the best result that looks closest to the ground truth.

### 4.3. Real to abstract translation

We then implement our proposed DRPAN on two tasks of real to abstract translation which requires many-to-one abstraction ability.

**Real to semantic labels.** For real to semantic labels task, we tested our DRPAN model on two of the most used

Method	PSNR(dB)	SSIM	VIF	RECO
L2+CGAN	22.19	0.8083	0.3640	-
ID-CGAN [41]	22.91	0.8198	0.3885	-
PAN [36]	23.35	0.8303	0.4050	-
DRPAN(without mask)	25.51	0.8688	0.4923	0.9670
DRPAN(128)	25.87	0.8714	0.4818	1.0770
DRPAN(64)	25.76	0.8765	0.4962	<b>1.1072</b>
DRPAN(32)	25.92	<b>0.8788</b>	<b>0.5001</b>	1.1067
DRPAN(16)	<b>26.20</b>	0.8712	0.4783	1.0875

Table 1: Quantitative comparison of our DRPAN (with different sizes of discriminative region) with ID-CGAN [41] and PAN [36] on image de-raining task. DRPAN performs best (in bold font) evaluated by PSNR, SSIM, VIF, and RECO metrics.

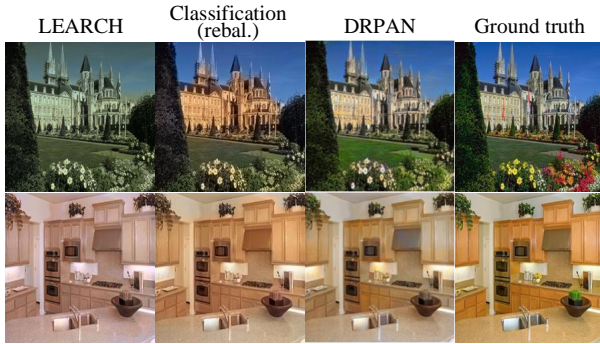


Figure 6: Example results of our DRPAN compared to LEARCH [8] and Classification (rebal.) [42] on image colorization task.

Model	Per-pixel acc.	Per-class acc.	Class IOU
L1+U-Net [14]	0.86	0.42	0.35
Pix2pix [14]	0.83	0.36	0.29
DRPAN	<b>0.88</b>	<b>0.52</b>	<b>0.43</b>

Table 2: Quantitative comparison of our DRPAN with Pix2pix [14] on real to semantic labels task. DRPAN performs best (in bold font) evaluated by per-pixel accuracy, per-class accuracy, and Class IOU.

datasets: Cityscapes and facades. Fig. 7 shows the qualitative results of our DRPAN compared to Pix2pix [14] on Cityscapes dataset for translating real to semantic labels, and DRPAN can synthesize more realistic results that are closer to ground truth than Pix2pix, meanwhile, the quantitative results in Tab. 2 can also tell this in terms of per-pixel accuracy, per-class accuracy, and Class IOU.

**Aerial to maps.** We also apply our DRPAN on aerial photo to maps task, and the experiment was implemented using paired images with  $512 \times 512$  resolution [14]. The top row of Fig. 8 shows the qualitative results of our DRPAN compared to Pix2pix [14], and it can be seen that our DR-

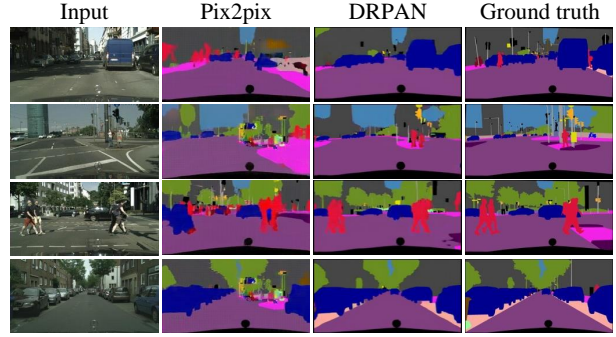


Figure 7: Example results of our DRPAN compared to Pix2pix [14] on real to semantic labels task.



Figure 8: Example results of our DRPAN compared to Pix2pix [14] on aerial to maps (top) and maps to aerial (bottom) tasks.

PAN can correctly translate the motorway on aerial photo into the orange line on the map while Pix2pix can't.

#### 4.4. Abstract to real translation

Besides, we also demonstrate our proposed DRPAN on several abstract to real tasks that can translate one to many: semantic labels to photo, maps to aerial, edge to real, and sketch to real.

**Semantic labels to real.** For semantic labels to real task, the translation model aims to synthesize real world images from semantic labels. CGAN based works fail to capture the details in the real world and suffer from deformation and blur problems. CNN based methods such as CRN can synthesize high-resolution but smooth rather than realistic results. Fig. 9 shows qualitative comparison of results, from which it can be seen that our DRPAN can synthesize the most realistic results with high-quality (more clear and less distorted while high resolution) compared to Pix2pix [14] and CRN [5]. The inception score on Cityscapes and facades datasets in Tab. 3 also validates that our DRPAN performs better than Pix2pix.



Figure 9: Example results of our DRPAN compared to Pix2pix [14] and CRN [5] on semantic labels to real task.

Model	Pix2pix [14]	DRPAN	Real data
Score $\pm$ std(Cityscapes)	2.35 $\pm$ 0.13	2.53 $\pm$ 0.25	2.71 $\pm$ 0.19
Score $\pm$ std(facades)	1.60 $\pm$ 0.25	1.67 $\pm$ 0.23	2.06 $\pm$ 0.23

Table 3: Quantitative comparison of our DRPAN with Pix2pix [14] on semantic labels to real task by inception score.

The evaluation of GAN is still a challenging problem. Many works [31, 37, 42, 14] used FCN-8s as automatic

measures of synthesized images. Tab. 4 reports performance evaluation on segmentation of FCN-8s model, and our DRPAN exceeds Pix2pix [14] by 10% on per-pixel accuracy and also achieves highest performance on per-class accuracy and Class IOU.

**Maps to aerial.** As opposed to aerial to maps task, we also tested our DRPAN on maps to aerial task, and the qualitative results are shown in the bottom row of Fig. 8, which clearly demonstrates that our DRPAN can synthesize higher quality aerial photos than Pix2pix [14].



Model	Per-pixel acc.	Per-class acc.	Class IOU
L1	0.44	0.14	0.10
cGAN	0.61	0.21	0.16
L1+GAN	0.64	0.19	0.15
L1+cGAN [14]	0.63	0.21	0.16
DRPAN	<b>0.73</b>	<b>0.24</b>	<b>0.19</b>
Ground truth	0.80	0.26	0.21

Table 4: Quantitative comparison of our DRPAN with other models on semantic labels to real task (Cityscapes dataset) by FCN-8s score.

Model	% Turkers labeled real
Pix2pix [14] against real	3.3%
CRN [5] against real	9.4%
DRPAN against real	<b>18.2%</b>
	% Turkers labeled more realistic
DRPAN vs. Pix2pix [14]	<b>95.2%</b>
DRPAN vs. CRN [5]	<b>75.7%</b>

Table 5: AMT real vs. fake results test on Cityscapes semantic labels to photo task.

Model	% Turkers labeled real
Pix2pix [14]	18.7%
CycleGAN [44]	26.8%
DRPAN	<b>39.0%</b>

Table 6: AMT real vs. fake results test on maps to aerial task.

**Human perceptual validation.** We assess the performance of abstract to real on semantic labels to photo and maps to aerial by AMT. For fake against real study, we followed the perceptual study protocol from [14], and collected data of each algorithm from 30 participants. Every participant has 1000ms to look one sample. We also compare how realistic the synthesized images between different algorithms. Tab. 5 illustrates that images synthesized by DRPAN were rated more realistic than state-of-the-arts (DRPAN 18.2% > CRN 9.4% > Pix2pix 3.3%), it also can be shown that, compared to Pix2pix [14], images synthesized by DRPAN were rated more realistic by 95.2%, and compared to CRN [5], DRPAN was rated more realistic by 75.7%. Tab. 6 reports the comparison on maps to aerial task and our DRPAN fooled participants on 39.0% over 18.7% of Pix2pix and 26.8% of CycleGAN [44].

**Edges to real and sketch to real.** For the edge to real and sketch to real tasks, previous works often encounter two problems [14]: one is that it’s easy to generate artifacts and artificial color distribution in regions when the input such as edge is sparse; the other is that it’s difficult to deal with unusual inputs like sketch. We tested our DRPAN model on UT Zappos50k dataset [40] and edge to handbag dataset [45]. Fig. 10 shows that our model can handle these

two problems better than Pix2pix.

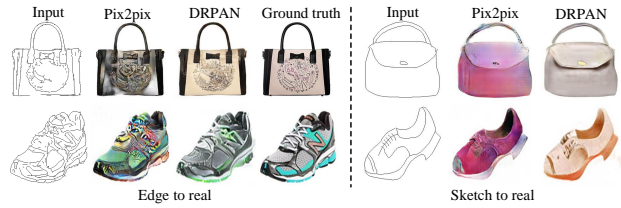


Figure 10: Example results of our DRPAN compared to Pix2pix [14] on edge to real (left) and sketch to real (right) tasks.

#### 4.5. Without or with fake-mask

Finally, we investigate the value of our proposed fake-mask operation for image-to-image translation tasks, and the results are shown in Fig. 11. It can be seen that, DRPAN with fake-mask can achieve better performance than DRPAN without fake-mask on several translation tasks, which can synthesize high-quality images with more reality and less distortion.

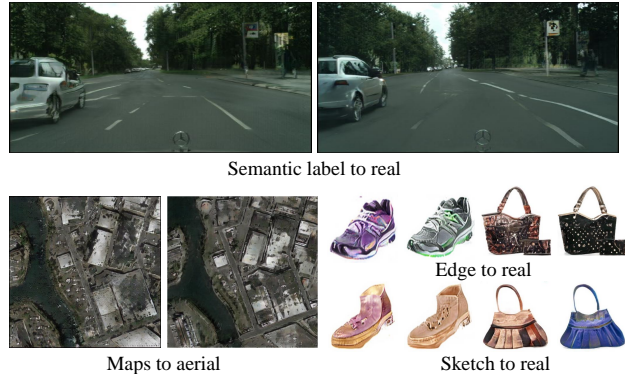


Figure 11: Example results of our DRPAN without (left) and with (right) fake-mask operation on several image-to-image translation tasks.

## 5. Conclusion

We propose Discriminative Region Proposal Adversarial Networks (DRPANs) towards high-resolution and photo-reality image-to-image translation. Human perceptual studies and automatic quantitative measures validate the performance of our proposed DRPAN against the state-of-the-arts for synthesizing high-quality results. We hope it can be explored for discriminative feature learning and other computer vision tasks in the future.



## References

- [1] M. Arjovsky, S. Chintala, and L. Bottou. Wasserstein gan. In *ICML*, 2017. 2, 4
- [2] S. Arora, R. Ge, Y. Liang, T. Ma, and Y. Zhang. Generalization and equilibrium in generative adversarial nets (GANs). *arXiv preprint arXiv:1703.00573*, 2017. 4
- [3] V. Baroncini, L. Capodiferro, E. D. Di Claudio, and G. Jaccovitti. The polar edge coherence: a quasi blind metric for video quality assessment. In *ESPC*, 2009. 5
- [4] L. Chen, G. Papandreou, I. Kokkinos, K. Murphy, and A. L. Yuille. Semantic image segmentation with deep convolutional nets and fully connected CRFs. In *ICLR*, 2015. 2
- [5] Q. Chen and V. Koltun. Photographic image synthesis with cascaded refinement networks. In *ICCV*, 2017. 2, 6, 7, 8
- [6] M. Cordts, M. Omran, S. Ramos, T. Rehfeld, M. Enzweiler, R. Benenson, U. Franke, S. Roth, and B. Schiele. The cityscapes dataset for semantic urban scene understanding. In *CVPR*, 2016. 1, 5
- [7] J. Deng, W. Dong, R. Socher, L.-J. Li, K. Li, and L. Fei-Fei. Imagenet: A large-scale hierarchical image database. In *CVPR*, 2009. 5
- [8] A. Deshpande, J. Rock, and D. Forsyth. Learning large-scale automatic image colorization. In *ICCV*, 2015. 2, 5, 6
- [9] C. Dong, C. C. Loy, K. He, and X. Tang. Image super-resolution using deep convolutional networks. *IEEE TPAMI*, 38(2):295–307, 2016. 1, 2
- [10] L. A. Gatys, A. S. Ecker, and M. Bethge. A neural algorithm of artistic style. *arXiv preprint arXiv:1508.06576*, 2015. 2
- [11] I. Goodfellow, J. Pougetabadie, M. Mirza, B. Xu, D. Wardefarley, S. Ozair, A. Courville, and Y. Bengio. Generative adversarial nets. In *NIPS*, 2014. 2
- [12] I. Gulrajani, F. Ahmed, M. Arjovsky, V. Dumoulin, and A. Courville. Improved training of Wasserstein GANs. *arXiv preprint arXiv:1704.00028*, 2017. 2, 4
- [13] S. Ioffe and C. Szegedy. Batch normalization: Accelerating deep network training by reducing internal covariate shift. In *ICML*, 2015. 4
- [14] P. Isola, J. Y. Zhu, T. Zhou, and A. A. Efros. Image-to-image translation with conditional adversarial networks. In *CVPR*, 2017. 1, 2, 4, 5, 6, 7, 8
- [15] J. Johnson, A. Alahi, and L. Fei-Fei. Perceptual losses for real-time style transfer and super-resolution. In *ECCV*, 2016. 2
- [16] J. Kim, J. K. Lee, and K. M. Lee. Accurate image super-resolution using very deep convolutional networks. In *CVPR*, 2016. 2
- [17] T. Kim, M. Cha, H. Kim, J. Lee, and J. Kim. Learning to discover cross-domain relations with generative adversarial networks. *arXiv preprint arXiv:1703.05192*, 2017. 2
- [18] N. Kodali, J. Abernethy, J. Hays, and Z. Kira. How to train your DRAGAN. *arXiv preprint arXiv:1705.07215*, 2017. 2, 4
- [19] C. Ledig, L. Theis, F. Huszar, J. Caballero, A. Cunningham, A. Acosta, A. Aitken, A. Tejani, J. Totz, and Z. Wang. Photo-realistic single image super-resolution using a generative adversarial network. In *CVPR*, 2017. 2, 4
- [20] C. Li and M. Wand. Precomputed real-time texture synthesis with markovian generative adversarial networks. In *ECCV*, 2016. 2, 4
- [21] Y. Li, S. Liu, J. Yang, and M. H. Yang. Generative face completion. In *CVPR*, 2017. 2
- [22] G. Lin, A. Milan, C. Shen, and I. Reid. Refinenet: Multi-path refinement networks for high-resolution semantic segmentation. In *CVPR*, 2017. 2
- [23] J. Long, E. Shelhamer, and T. Darrell. Fully convolutional networks for semantic segmentation. In *CVPR*, 2015. 1, 2, 5
- [24] V. Nair and G. E. Hinton. Rectified linear units improve restricted boltzmann machines. In *ICML*, 2010. 4
- [25] A. Nguyen, J. Clune, Y. Bengio, A. Dosovitskiy, and J. Yosinski. Plug & play generative networks: Conditional iterative generation of images in latent space. In *CVPR*, 2017. 2
- [26] D. Pathak, P. Krahenbuhl, J. Donahue, T. Darrell, and A. A. Efros. Context encoders: Feature learning by inpainting. In *CVPR*, 2016. 2
- [27] G.-J. Qi. Loss-sensitive generative adversarial networks on lipschitz densities. *arXiv preprint arXiv:1701.06264*, 2017. 2, 4
- [28] A. Radford, L. Metz, and S. Chintala. Unsupervised representation learning with deep convolutional generative adversarial networks. In *ICLR*, 2016. 2, 4
- [29] S. Reed, Z. Akata, X. Yan, L. Logeswaran, B. Schiele, and H. Lee. Generative adversarial text to image synthesis. In *ICML*, 2016. 2
- [30] O. Ronneberger, P. Fischer, and T. Brox. U-Net: Convolutional networks for biomedical image segmentation. In *MICCAI*, 2015. 2
- [31] T. Salimans, I. Goodfellow, W. Zaremba, V. Cheung, A. Radford, and X. Chen. Improved techniques for training gans. In *NIPS*, 2016. 5, 7
- [32] H. R. Sheikh and A. C. Bovik. Image information and visual quality. *IEEE TIP*, 15(2):430–444, 2006. 5
- [33] W. Shi, J. Caballero, F. Huszar, J. Totz, A. P. Aitken, R. Bishop, D. Rueckert, and Z. Wang. Real-time single image and video super-resolution using an efficient sub-pixel convolutional neural network. In *CVPR*, 2016. 2
- [34] A. Shrivastava, T. Pfister, O. Tuzel, J. Susskind, W. Wang, and R. Webb. Learning from simulated and unsupervised images through adversarial training. In *CVPR*, 2017. 2, 4, 5
- [35] R. Tyleček and R. Šára. Spatial pattern templates for recognition of objects with regular structure. In *GICPR*, 2013. 3
- [36] C. Wang, C. Xu, C. Wang, and D. Tao. Perceptual adversarial networks for image-to-image transformation. In *IJCAI*, 2017. 6
- [37] X. Wang and A. Gupta. Generative image modeling using style and structure adversarial networks. In *ECCV*, 2016. 2, 7
- [38] Z. Wang, A. C. Bovik, H. R. Sheikh, and E. P. Simoncelli. Image quality assessment: from error visibility to structural similarity. *IEEE TIP*, 13(4):600–612, 2004. 5
- [39] Z. Yi, H. Zhang, P. Tan, and M. Gong. DualGAN: Unsupervised dual learning for image-to-image translation. In *ICCV*, 2017. 2, 5

- [40] A. Yu and K. Grauman. Fine-Grained Visual Comparisons with Local Learning. In *CVPR*, 2014. 8
- [41] H. Zhang, V. Sindagi, and V. M. Patel. Image de-raining using a conditional generative adversarial network. In *CVPR*, 2017. 2, 5, 6
- [42] R. Zhang, P. Isola, and A. A. Efros. Colorful image colorization. In *ECCV*, 2016. 2, 6, 7
- [43] Z. Zheng, L. Zheng, and Y. Yang. Unlabeled samples generated by gan improve the person re-identification baseline in vitro. In *ICCV*, 2017. 5
- [44] J. Zhu, T. Park, P. Isola, and A. A. Efros. Unpaired image-to-image translation using cycle-consistent adversarial networks. In *ICCV*, 2017. 2, 4, 5, 8
- [45] J.-Y. Zhu, P. Krähenbühl, E. Shechtman, and A. A. Efros. Generative visual manipulation on the natural image manifold. In *ECCV*, 2016. 8